

Width and Magnetic Field Dependence of Transition Temperature in Ultranarrow Superconducting Wires

Robert A Smith¹, Beccy S Handy¹ and Vinay Ambegaokar²

¹ *School of Physics and Astronomy, University of Birmingham, Edgbaston, Birmingham B15 2TT, ENGLAND*

² *Laboratory of Atomic and Solid State Physics, Cornell University, Ithaca NY14853, USA*

We calculate the transition temperature in ultranarrow superconducting wires as a function of resistance, wire width and applied magnetic field. We compare the results of first-order perturbation theory and the non-perturbative resummation technique developed by Oreg and Finkel'stein. The latter technique is found to be superior as it is valid even in the strong disorder limit. In both cases, the predicted additional suppression of the transition temperature due to the reduced dimensionality is strongly dependent upon the boundary conditions used. When we use the correct (zero-gradient) boundary conditions, we obtain qualitative agreement between theory and experiment.

I. INTRODUCTION

Recent experiments on disordered superconducting wires¹⁻⁴ have led to renewed interest in the interplay of interaction and disorder in low-dimensional systems. These experiments have been made possible by the development of fabrication techniques using either stencils or carbon nanotubes, and involve wires of width as low as 50Å and thickness as low as 10Å. An obvious question to ask in such systems is how the transition temperature is affected by wire width and thickness. Decreasing the thickness of the wire increases the normal state resistance per square which is a measure of the amount of disorder in the system. This increase in disorder reduces the transition temperature for reasons we discuss later. Decreasing the width of the wire leads to a crossover from two- to one-dimensional behavior, where increased fluctuation effects further reduce the transition temperature. Ultimately the combined disorder and fluctuation effects completely suppress superconductivity, and a superconductor-insulator transition results⁶. The effect of dimensionality on this quantum phase transition is obviously very interesting from a theoretical point of view. As a first step to understanding this transition, we will compare predictions of transition temperature to experimental results. Unfortunately there is very little data available for comparison because each data point requires the fabrication of a new wire which is very costly in terms of experimental effort. We therefore suggest the application of a magnetic field as a way to generate more data points for each wire and make predictions for this effect.

The most basic model used⁷⁻⁹, which is generally believed in, consists of electrons moving in a disordered background interacting via the Coulomb repulsion and a featureless phonon-mediated attraction. Simple as this model is, significant difficulties arise even when calculating the suppression of transition temperature in two-dimensional films. These difficulties will be compounded when looking at quasi one-dimensional wires, which are in a crossover regime, so it is most important that they are fully understood in the simpler two-dimensional case. The basic physics involved is not in dispute, and can be understood from the BCS-MacMillan formula for the transition temperature, T_c ,

$$T_c = 1.13\omega_D \exp\left(-\frac{1}{N(0)[\gamma - \mu^*]}\right), \quad (1)$$

where ω_D is the Debye frequency (a typical phonon frequency), $N(0)$ is the electronic density of states per spin at the Fermi surface, γ is the featureless attraction, and μ^* is the Coulomb pseudopotential, a measure of the Coulomb repulsion. The disorder causes the electrons to move diffusively rather than ballistically making them less efficient at screening the Coulomb repulsion. This increases μ^* and decreases $N(0)$, both effects leading to a decrease in T_c . We shall assume that the disorder does not affect phonon properties such as ω_D and γ , an assumption that is backed up by detailed calculation on at least one model of electron-phonon interaction¹⁰. Other authors¹¹ have questioned this assumption, and we intend to address this point in future work.

The first difficulty which occurs in two dimensions relates to the low-momentum singularity of the disorder-screened Coulomb potential, which is given by

$$V_C(q, \omega_m) = \frac{4\pi e^2}{q^2} \frac{Dq^2 + |\omega_m|}{Dq_{TF}^2 + Dq^2 + |\omega_m|} \approx \frac{1}{2N(0)} \frac{Dq^2 + |\omega_m|}{Dq^2}, \quad (2)$$

where q_{TF} is the Thomas-Fermi screening wavenumber defined by $q_{TF}^2 = 8\pi e^2 N(0)$, $D = v_F^2 \tau / 2$ is the diffusion constant, v_F is the Fermi velocity, and τ is the elastic scattering time. This singularity leads to a strong suppression

of the one-particle density of states¹² which is seen experimentally in tunneling measurements¹³. Naively inserting this density of states into Eqn. [1] predicts a large suppression of T_c which is not seen experimentally. This prediction is, in fact, incorrect due to a cancellation^{8,9} between the various diagrammatic contributions in perturbation theory. The apparently mysterious cancellation turns out to be due to gauge invariance¹⁴ and is thus expected to be a very robust phenomenon. The end result is that the Coulomb interaction is effectively featureless with strength $N(0)V_C = 1/2$. The fact that we can legitimately use a featureless interaction makes calculations much simpler. Our first task is therefore to check that this replacement is still valid in quasi-1D systems.

The other difficulty is that perturbation theory cannot take us to the superconductor-insulator transition as it is only valid for weak disorder, and *ad hoc* attempts to extend its range of validity lead to unphysical reentrance problems. Oreg and Finkel'stein¹⁵ overcame this problem by developing a resummation technique, which has recently been shown to be related to strong-coupling theory¹⁶. We shall reexamine their predictions for wires and extend their approach to include the effect of a magnetic field. Rather surprisingly we find that the problem is extremely sensitive to the boundary conditions used. We argue that the physically correct boundary conditions are zero-gradient ones.

The remainder of the paper is organised in the following manner. In section (II) we consider first-order perturbation theory in the absence of a magnetic field. This is the simplest approach possible, and we will use it as a testing ground for the validity of the approximations used. Specifically we will show that it is legitimate to use a featureless Coulomb interaction and ignore self-energy effects, but that the details of boundary conditions are important. In section (III) we make predictions for the transition temperature using the resummation technique, all the necessary approximations having been justified in section (II). We then compare theory and experiment and find qualitative but not quantitative agreement. In section (IV) we consider the effect of an applied magnetic field on the transition temperature. The dimensions of the wires are such that we must consider both orbital and Zeeman (spin) effects¹⁹. As yet there is no experimental data available for comparison to the theory.

II. FIRST ORDER PERTURBATION THEORY

We will now calculate the transition temperature, T_c , which we identify as the temperature at which the pair propagator, $L(q, \Omega = 0)$, diverges. The latter is defined in Fig. 1(a) in terms of the BCS interaction, γ , and the pair polarization function, $P(q, 0)$, by

$$L(q, 0)^{-1} = \gamma^{-1} - P(q, 0). \quad (3)$$

Let us first consider mean field theory, which corresponds to zeroth order in disorder perturbation theory, for which the expansion parameter is $1/k_F\ell$, where k_F is the Fermi wavenumber and $\ell = v_F\tau$ is the elastic mean free path. The mean field pair polarization function is shown in Fig. 1(b), and leads to the pair propagator

$$L_0(q, 0)^{-1} = N(0) \left[\ln \left(\frac{T}{T_{c0}} \right) + \psi \left(\frac{1}{2} + \frac{Dq^2}{4\pi T} \right) - \psi \left(\frac{1}{2} \right) \right]. \quad (4)$$

The first-order perturbative corrections to the pair polarization function, $\delta P(q, 0)$, are shown in Fig. 1(c), and lead to a suppression in transition temperature

$$\ln \left(\frac{T_c}{T_{c0}} \right) = \frac{\delta P(q, 0)}{N(0)}. \quad (5)$$

Note that we evaluate the pair propagator at non-zero external momentum, q , since we will eventually consider the effect of a magnetic field.

The five diagrams of Fig. 1(c) can be understood in physical terms: diagrams 1 and 2 are self-energy diagrams and give corrections to the electronic density of states, $N(0)$; diagrams 3 and 4 are pseudopotential diagrams and give corrections to the effective Coulomb repulsion, μ^* ; diagram 5 involves the effect of Coulomb interaction on superconducting fluctuations. We will first perform the calculations exactly, and demonstrate the cancellation of the low-momentum singularity in the Coulomb interaction which occurs between diagrams 1–4 and 5. We show that this is equivalent to considering only diagrams 1–4 with a featureless Coulomb interaction of strength $N(0)V_C = 1/2$. In other words, the only purpose of diagram 5 is to remove the low-momentum singularity, as required by gauge invariance. Finally we show that the self-energy diagrams 1 and 2 can be ignored as they give a much smaller contribution than diagrams 3 and 4. The contributions from the five diagrams are as follows:

$$\begin{aligned}
\delta P_1 &= -4\pi N(0)T \sum_{\epsilon_l} T \sum_{\omega_m} \frac{1}{aL} \sum_{q'} \frac{Dq^2 + Dq'^2 + 3|\epsilon_l| + |\epsilon_l + \omega_m|}{(Dq^2 + 2|\epsilon_l|)^2 (Dq'^2 + |\epsilon_l| + |\epsilon_l + \omega_m|)^2} V_C(q', |\omega_m|) \theta(-\epsilon_l(\epsilon_l + \omega_m)) \\
\delta P_2 &= 4\pi N(0)T \sum_{\epsilon_l} T \sum_{\omega_m} \frac{1}{aL} \sum_{q'} \frac{1}{(Dq^2 + 2|\epsilon_l|)^2 (D(q' + q)^2 + |\epsilon_l| + |\epsilon_l + \omega_m|)} V_C(q', |\omega_m|) \theta(\epsilon_l(\epsilon_l + \omega_m)) \\
\delta P_3 &= -4\pi N(0)T \sum_{\epsilon_l} T \sum_{\omega_m} \frac{1}{aL} \sum_{q'} \frac{Dq^2 + Dq'^2 + |\epsilon_l| + |\epsilon_l + \omega_m|}{(Dq^2 + 2|\epsilon_l|)(Dq^2 + 2|\epsilon_l + \omega_m|)(Dq'^2 + |\epsilon_l| + |\epsilon_l + \omega_m|)^2} V_C(q', |\omega_m|) \theta(-\epsilon_l(\epsilon_l + \omega_m)) \\
\delta P_4 &= -4\pi N(0)T \sum_{\epsilon_l} T \sum_{\omega_m} \frac{1}{aL} \sum_{q'} \frac{1}{(Dq^2 + 2|\epsilon_l|)(Dq^2 + 2|\epsilon_l + \omega_m|)(D(q' + q)^2 + |\epsilon_l| + |\epsilon_l + \omega_m|)} V_C(q', |\omega_m|) \theta(\epsilon_l(\epsilon_l + \omega_m)) \\
\delta P_5 &= 4\pi^2 N(0)^2 T \sum_{\omega_m} \frac{1}{aL} \sum_{q'} \left[T \sum_{\epsilon_l} \left\{ \frac{|\omega_m|}{(Dq^2 + 2|\epsilon_l|)(Dq^2 + 2|\epsilon_l + \omega_m|)(D(q + q')^2 + |\epsilon_l| + |\epsilon_l + \omega_m|)} \theta(\epsilon_l(\epsilon_l + \omega_m)) \right. \right. \\
&\quad \left. \left. + \frac{Dq^2 + |\omega_m|}{(Dq^2 + 2|\epsilon_l|)(Dq^2 + 2|\epsilon_l + \omega_m|)(D(q + q')^2 + |\epsilon_l| + |\epsilon_l + \omega_m|)} \theta(-\epsilon_l(\epsilon_l + \omega_m)) \right\} \right]^2 V_C(q', |\omega_m|) L(q + q', |\omega_m|) \quad (6)
\end{aligned}$$

where $\epsilon_l = (2l + 1)\pi T$ is a Fermi Matsubara frequency and $\omega_m = 2m\pi T$ is a Bose Matsubara frequency. The diffusive form of the denominators in Eqn. (6) is valid only for momentum and frequency values such that Dq'^2 , $|\epsilon_l|$, $|\omega_m| < 1/\tau$, so we introduce the upper cutoff, $1/\tau$, in all these sums.

For the rest of this section we will work at zero magnetic field, so we set $q = 0$. The terms δP_{1-5} have previously been summed for 2D films⁹ to give the expression

$$\begin{aligned}
\ln\left(\frac{T_c}{T_{c0}}\right) &= -T \sum_{\omega_m} \frac{1}{aL} \sum_{q'} \left\{ -\frac{1}{2\pi T} \frac{Dq'^2}{\omega_m^2 - (Dq'^2)^2} \psi'\left(\frac{1}{2} + \frac{\omega_m}{2\pi T}\right) + \frac{2Dq'^2[\omega_m^2 + (Dq'^2)^2]}{\omega_m[\omega_m^2 - (Dq'^2)^2]^2} \left[\psi\left(\frac{1}{2} + \frac{\omega_m}{2\pi T}\right) - \psi\left(\frac{1}{2}\right) \right] \right. \\
&\quad \left. - \frac{4(Dq'^2)^2}{[\omega_m^2 - (Dq'^2)^2]^2} \frac{\left[\psi\left(\frac{1}{2} + \frac{\omega_m}{2\pi T}\right) - \psi\left(\frac{1}{2}\right) \right]^2}{\left[\psi\left(\frac{1}{2} + \frac{Dq'^2 + \omega_m}{4\pi T}\right) - \psi\left(\frac{1}{2}\right) \right]} \right\} V_C(q', \omega_m) \quad (7)
\end{aligned}$$

The $1/q'^2$ singularity in the screened Coulomb potential $V_C(q', \omega_m)$ is cancelled since there is an overall factor of Dq'^2 in the above equation. Note that there is, in fact, no divergence at $Dq'^2 = \omega_m$, but this can only be seen by Taylor expanding to second order. The need to perform this expansion makes the calculation involved, especially at the level of numerics. To allow simplification, we define $y = Dq'^2/2\pi T$ and $m = \omega_m/2\pi T$, which leads to the result

$$\begin{aligned}
\ln\left(\frac{T_c}{T_{c0}}\right) &= -\frac{1}{4\pi^2 N(0)T} \sum_{m=1}^M \frac{1}{aL} \sum_{q'} \left[\left\{ \frac{2}{m} \left[\psi\left(\frac{1}{2} + m\right) - \psi\left(\frac{1}{2}\right) \right] + \psi'\left(\frac{1}{2} + m\right) \right\} \frac{1}{y + m} \right. \\
&\quad \left. - \frac{4y}{(m + y)(m - y)^2} \left\{ \frac{\left[\psi\left(\frac{1}{2} + m\right) - \psi\left(\frac{1}{2}\right) \right]^2}{\left[\psi\left(\frac{1}{2} + \frac{m + y}{2}\right) - \psi\left(\frac{1}{2}\right) \right]} - \left[\psi\left(\frac{1}{2} + m\right) - \psi\left(\frac{1}{2}\right) \right] + \frac{1}{2}(y - m)\psi'\left(\frac{1}{2} + m\right) \right\} \right] \quad (8)
\end{aligned}$$

where we have split off the most divergent term at large momentum and frequency, and $M = 1/2\pi T\tau$. To proceed further we must consider the q' -sum in various dimensions. In two dimensions the sum becomes an integral, and it is most sensible to perform the cut-off in a circularly symmetric manner

$$\frac{1}{aL} \sum_{q'} \mapsto \int_0^{1/\tau} \frac{2\pi q' dq'}{(2\pi)^2} = \frac{T}{2D} \int_0^M dy. \quad (9)$$

In quasi-1D wires, we must replace the integral in the transverse direction by a sum,

$$\frac{1}{aL} \sum_{q'} \mapsto \frac{1}{a} \sum_{q'_a} \int_0^{1/\tau} \frac{dq'_L}{2\pi}, \quad (10)$$

where $q'^2 = q_L'^2 + q_a'^2$. At this point we have to decide which boundary conditions to use in the transverse direction. To illustrate the strong effect this has we will compare three different boundary conditions: periodic and zero-gradient boundary conditions, whose physical origin is clear, and the boundary conditions used by Oreg and Finkel'stein. The details of all the boundary conditions are listed in Table 1. We note that the Oreg-Finkel'stein boundary conditions are equivalent to zero-gradient ones if the width, a , is replaced by $a/2$. The zero-gradient boundary conditions are the physically correct ones for a superconductor-insulator boundary as discussed in Ref. [17]. To perform the sum over q' note that we can write $y = y_L + y_a$ where $y_L = Dq_L'^2/2\pi T$ and $y_a = Dq_a'^2/2\pi T$, and if we define $z = \sqrt{y_L}$, the q'_L -integral becomes

$$\int_0^{1/\tau} \frac{dq'_L}{2\pi} = \int_0^{\sqrt{M}} \frac{dz}{L_T}. \quad (11)$$

where $L_T = \sqrt{2\pi D/T}$ is the thermal length. Note that $y = z^2 + 4p(a/L_T)^2$ for zero-gradient boundary conditions and $y = z^2 + p(a/L_T)^2$ for the other two types. The final result of perturbation theory is then given by Eqn. (8) with the prefactor and sums becoming

$$-\frac{1}{4\pi^2 N(0)T} \sum_{m=1}^M \sum_{q'} \mapsto \begin{cases} -t \sum_{m=1}^M \int_0^M dy & \text{2D} \\ -\frac{t}{\pi} \left(\frac{L_T}{a}\right) \sum_{m=1}^M \sum_p \int_0^{\sqrt{M}} & \text{quasi-1D} \end{cases} \quad (12)$$

In the above, t is a dimensionless measure of disorder given by

$$t = \frac{1}{8\pi^2 N(0)D} = \frac{R_{\square}}{R_0} \quad (13)$$

where R_{\square} is the normal state resistance per square, and $R_0 = 2\pi h/e^2 \approx 162k\Omega$. Note that t only differs from the previously discussed parameter $1/k_F \ell$ by a factor 2π .

Having shown that the low-momentum singularity in the screened Coulomb potential is cancelled by diagram 5, we recalculate the suppression of transition temperature using a featureless Coulomb potential of magnitude $N(0)V_C = 1/2$, and including only diagrams 1-4. We have previously shown¹⁸ that the above equations simplify to give

$$\begin{aligned} \delta P_{12} &= -T \sum_{\omega_m > 0} \left[\psi \left(\frac{1}{2} + \frac{\omega_m}{2\pi T} \right) - \psi \left(\frac{1}{2} \right) \right] \sum_{q'} \frac{1}{(Dq'^2 + \omega_m)^2} \\ \delta P_{34} &= -2T \sum_{\omega_m > 0} \left[\psi \left(\frac{1}{2} + \frac{\omega_m}{2\pi T} \right) - \psi \left(\frac{1}{2} \right) \right] \frac{1}{\omega_m} \sum_{q'} \frac{1}{(Dq'^2 + \omega_m)}. \end{aligned} \quad (14)$$

For convenience we define dimensionless sums $I_1(m)$ and $I_2(m)$ as

$$\begin{aligned} I_1(m) &\equiv \frac{4\pi D}{aL} \sum_{q'} \frac{1}{Dq'^2 + |\omega_m|} \\ I_2(m) &\equiv \frac{4\pi D}{aL} \sum_{q'} \frac{2\pi T}{(Dq'^2 + |\omega_m|)^2} \end{aligned} \quad (15)$$

which are evaluated in two dimensions and quasi-one dimension in Appendix A. When we combine Eqns. (5) and (14) we obtain the formula for transition temperature suppression assuming a featureless Coulomb potential,

$$\ln \left(\frac{T_c}{T_{c0}} \right) = -t \sum_{m=1}^M \left[\psi \left(\frac{1}{2} + m \right) - \psi \left(\frac{1}{2} \right) \right] \left[I_2(m) + \frac{2I_1(m)}{m} \right]. \quad (16)$$

The contribution of the pseudopotential diagrams (δP_{34}) is found to be much larger than that of the self-energy diagrams (δP_{12}), so that we can ignore the term $I_2(m)$ in the above equation.

We will now numerically confirm the statements we have made previously concerning the effective featurelessness of the Coulomb interaction and the strong sensitivity to boundary conditions. First we compare the results of the

exact calculation for transition temperature (correctly screened Coulomb potential and all first-order diagrams) with those of the approximate calculations (featureless Coulomb potential and restricted set of diagrams). The same (zero-gradient) boundary conditions are used throughout, and the results are shown in Fig. 2. Although a slight difference can be seen between the three plots, this vanishes when we fit the initial slope of the $T_c(R_{\square})$ curve to experiment, which sets the value of M , the upper cut-off in Matsubara sums. The relative suppression of transition temperature due to decreasing wire width is thus found to be independent of how the Coulomb potential is treated. This demonstrates that the simplest approach – featureless Coulomb potential and no self-energy diagrams – is valid. This is important since these simplifications are necessary for the resummation technique.

Next we compare the effects of different boundary conditions on the predicted suppression of transition temperature. All calculations are made using a featureless Coulomb potential and the results are plotted in Fig. 3. Rather surprisingly, we see a very strong dependence on the boundary conditions used, which we believe is due to the difference in relative magnitude of the zero mode in each case. The periodic boundary condition curves do not show a trend with decreasing wire width, whilst the boundary conditions used by Oreg and Finkel'stein yield a stronger suppression than the zero-gradient boundary conditions as wire width has effectively been halved in the former case. We note that if wire width, a , and thermal length, L_T , are known, then it is important to use zero-gradient rather than Oreg-Finkel'stein boundary conditions. On the other hand, if the ratio a/L_T is a fitting parameter, then the two boundary conditions yield identical results.

To summarise, our main observation is the large sensitivity of the result to the boundary conditions used, and the need to use the correct zero-gradient ones. The results are not very sensitive to either the form of the Coulomb interaction used, or the inclusion of self-energy corrections, and so we are free to choose whichever approach we prefer. Finally we note that in all figures the perturbative curves suffer from re-entrance problems at low temperature, so that there is no prediction for T_c beyond a certain value of R_{\square} . This unphysical behaviour is solved using the resummation technique, as discussed in the next section.

III. THE RESUMMATION TECHNIQUE

In this section we will review the resummation technique¹⁵ developed by Oreg and Finkel'stein (OF) as applied to the problem of T_c suppression in quasi-1D wires. This method involves calculating the pair-amplitude, $\Gamma(\epsilon_n, \epsilon_l)$, which is a matrix with Fermi Matsubara frequencies labelling its rows and columns. The transition temperature is identified as the temperature at which this matrix becomes singular. OF obtained an equation for Γ by including only pseudopotential diagrams, and solved it using matrix perturbation theory with the set of boundary conditions described in Table 1. We have performed calculations to show that it is legitimate to include only these diagrams, but that it is essential to use zero-gradient boundary conditions. These results are not shown here as the effects are virtually identical to those seen in perturbation theory. In a previous paper¹⁸ we have shown that the equation for Γ can be solved exactly at no extra numerical cost, so the matrix perturbation theory is unnecessary. Therefore we shall include only pseudopotential diagrams but solve the equation for Γ using an exact diagonalization method with the correct boundary conditions.

Before we proceed further, let us briefly describe the details of the technique. The ladder summation involved is shown in Fig. 4. The block $t\Lambda$, an effective Coulomb pseudopotential, contains diagrams 3 and 4 of Fig. 1(c); the block Σ , the self-energy of the Cooperon impurity ladder, C , contains diagrams 1 and 2 of Fig. 1(c). We have included the self-energy diagrams for completeness, although their effects can be ignored in calculations, as discussed above. The equation for Γ is seen to be

$$\Gamma(\epsilon_n, \epsilon_l) = -|\gamma| + t\Lambda(\epsilon_n, \epsilon_l) - 2\pi T \sum_{m=0}^M [-|\gamma| + t\Lambda(\epsilon_n, \epsilon_m)] \frac{1}{|\epsilon_m|} \Gamma(\epsilon_m, \epsilon_l) \quad (17)$$

where the contributions to $t\Lambda$ are

$$\begin{aligned} t\Lambda_3(\epsilon_n, \epsilon_m) &= \frac{1}{2\pi N(0)} \frac{1}{aL} \sum_{q'} \frac{Dq^2 + Dq'^2 + |\epsilon_n| + |\epsilon_m|}{[Dq'^2 + |\epsilon_n| + |\epsilon_m|]^2} \theta(-\epsilon_n \epsilon_m) \\ t\Lambda_4(\epsilon_n, \epsilon_m) &= \frac{1}{2\pi N(0)} \frac{1}{aL} \sum_{q'} \frac{1}{[Dq'^2 + |\epsilon_n| + |\epsilon_m|]} \theta(\epsilon_n \epsilon_m). \end{aligned} \quad (18)$$

We have kept non-zero external momentum q so that we can include magnetic field effects later. For now we consider the case of zero magnetic field, so we set $q = 0$, and the two contributions to $t\Lambda$ are identical. It follows that $\Lambda(\epsilon_n, \epsilon_m)$ does not depend upon the relative sign of ϵ_n and ϵ_m and has the form

$$\Lambda(\epsilon_n, \epsilon_m) = I_1(n + m + 1), \quad (19)$$

where I_1 is defined in Eqn. (15). Eqn. (17) can then be written in matrix form as

$$\hat{\Gamma} = -|\gamma|\hat{1} + t\hat{\Lambda} - [-|\gamma|\hat{1} + t\hat{\Lambda}] \hat{\epsilon}^{-1} \hat{\Gamma}, \quad (20)$$

where $\hat{\Gamma}_{nm} = \Gamma(\epsilon_n, \epsilon_m)$, $\hat{1}_{nm} = 1$, $\hat{\Lambda}_{nm} = \Lambda(\epsilon_n, \epsilon_m)$ and $\hat{\epsilon}_{nm} = (n + 1/2)\delta_{nm}$. This has the solution

$$\hat{\Gamma} = \hat{\epsilon}^{1/2} (\hat{I} - |\gamma|\hat{\Pi})^{-1} \hat{\epsilon}^{-1/2} (-|\gamma|\hat{1} + t\hat{\Lambda}), \quad (21)$$

where

$$\hat{\Pi} = \hat{\epsilon}^{-1/2} [\hat{1} - |\gamma|^{-1} t \hat{\Lambda}] \hat{\epsilon}^{-1/2}, \quad (22)$$

and $\hat{I}_{nm} = \delta_{nm}$ is the identity matrix. It follows that when the matrix $\hat{\Pi}$ has an eigenvalue equal to $1/|\gamma|$, the pair amplitude diverges, and we have found T_c . In other words, we need to solve the eigenvalue equation

$$\left[|\gamma|^{-1} \hat{I} - \hat{\Pi}(T_c) \right] |\psi\rangle = 0. \quad (23)$$

Of solve Eqn. (23) using the standard degenerate perturbation theory familiar from elementary quantum mechanics. On the other hand, we solve by diagonalizing the matrix $[|\gamma|^{-1} \hat{I} - \hat{\Pi}(T)]$ numerically, and decreasing the temperature until its lowest eigenvalue equals zero. Since we only need the lowest eigenvalue, and the matrix has such a simple structure, the Lanczos method is very efficient here. The only minor complication is that the matrix $\hat{\Pi}(T)$ depends upon T both through the dependence of $\hat{\Lambda}$ upon T and through its rank $M = 1/2\pi T\tau$. We therefore start at the mean-field value of M , which we will call M_0 , and decrease the temperature by increasing M successively by one. We diagonalize the matrix $[|\gamma|^{-1} \hat{I} - \hat{\Pi}]$ for each value of M until the lowest eigenvalue changes sign. At this point we have found T_c for the given problem, and $T_c/T_{c0} = M_0/M$. This is obviously the method of choice, since no approximation is involved. We compare the results of exact diagonalization and matrix perturbation theory in Fig. 5 to see if any major errors arise from the latter method. We find that although exact diagonalization and matrix perturbation theory agree at low values of resistance, they deviate at larger values. This is to be expected since the latter method is an expansion around T_{c0} , and at large values of resistance the actual T_c can be very much smaller than T_{c0} . From now on, therefore, we shall use the exact diagonalization method.

We can now compare theory and experiment, but we must first decide exactly what effect we wish to fit. The output from our theoretical analysis is $T_c(R_{\square}, a)/T_c(0, a)$, the relative suppression of T_c due to disorder, R_{\square} . The basic phenomenon we are focusing upon is the additional transition temperature suppression caused by decreasing wire width, which suggests that the quantity to examine is $T_c(R_{\square}, a)/T_c(R_{\square}, 2D)$. In fact we will consider the *additional relative* suppression,

$$\Theta(R_{\square}, a) = \frac{T_c(R_{\square}, a)/T_c(0, a)}{T_c(R_{\square}, 2D)/T_c(0, 2D)} \quad (24)$$

in order to overcome two difficulties. The first is that experiment and theory do not agree for some of the 2D films used. If we assume that this is due to some additional physical processes that will affect samples in the same manner independent of width, this unwanted effect factors out in the ratio Θ . The second difficulty is that wires of different widths do not appear to have the same value of T_c in the clean limit, $T_c(0, a)$. Again one could hope that this effect factors out, although there is the possibility that it might be due to a change in phonon spectrum or coupling, which could make the BCS $|\gamma|$ width-dependent. Also, given that experiments are often carried out on Pb, strong-coupling effects might need to be considered. However, the fact that extremely small superconductors usually have very similar T_c values to bulk superconductors of the same material suggests that phonon coupling is not strongly affected by the reduced dimensionality.

Having established which physical quantity we need to examine, the next thing to do is to see what experiments there are to fit. There are three sets of experimental data that we know about: those of Graybeal et al (1987)¹, Sharifi et al (1993)², and Xiong et al (1997)³. The data of Graybeal et al consists of T_c vs a for wires of constant thickness (and hence constant resistance per square). Their data shows that the relative suppression of T_c varies as $1/a^2$ with a proportionality constant independent of R_{\square} . We have performed calculations which predict a dependence roughly of the form $1/a$, but with a proportionality constant dependent on R_{\square} . We will therefore not consider this data further. The data of Sharifi et al and Xiong et al is plotted in the form of $T_c(R_{\square}, a)$ vs R_{\square} for different wires in Fig. 6. From this we see that only the data of Xiong et al shows a consistent trend with decreasing width, so it is

only this data that we shall attempt to fit. The fact that this is the most recent data is reassuring, since it suggests that more recent fabrication techniques have produced better quality wires.

In Fig. 7, we replot the data of Xiong et al in the form of $\Theta(R_{\square}, a)$ vs R_{\square} and compare to theory. In generating the theoretical data, we have assumed that the wire widths quoted in Xiong et al are correct, and we have used the value of the thermal length quoted in Sharifi et al (viz $L_T = 400\text{\AA}$ at $T = 4K$, which corresponds to $L_T = 300\text{\AA}$ at $T_{c0} = 6.9K$). The order of magnitude agreement is good, which would not have been the case had we used either periodic boundary conditions (which would give essentially no effect) or Oreg-Finkel'stein boundary conditions (which would give too large an effect for the same values of a/L_T). However, the detailed fit of theory to experiment is not good. This may have been anticipated by simply looking at the experimental points: the data does not show a smooth trend as width is decreased – the 580\AA , 350\AA and 250\AA wire data fall on top of each other, whilst the 1000\AA wire data shows essentially 2D behavior. The 2D to quasi-1D crossover is expected to occur when the width, a , is of the order of the thermal length, $L_T \approx 300\text{\AA}$, so the experiment shows the expected qualitative behavior. We note that the relatively small amount of data (19 points in total), which is due to the experimental difficulty involved, means that a systematic comparison to theory is currently impossible. What is needed is a method to generate more data points without having to make a new wire each time. Applying a magnetic field would appear to be a natural way to do this, and we therefore extend our theory to include the effect of such a field in the next section.

IV. EFFECT OF AN APPLIED MAGNETIC FIELD

We will now consider the effect of an applied perpendicular magnetic field. There are two effects to consider here: the *orbital* effect, caused by the magnetic field scrambling the relative phase of the electrons in a Cooper pair, and the *Zeeman* effect, caused by the magnetic field lifting the degeneracy of up and down spins. Let us first consider the relative importance of the two effects. The orbital effect will destroy superconductivity when the magnetic dephasing rate, $1/\tau_H$, is of the order of $k_B T_c$, which gives $H \approx 4T$ for a Pb wire of width 250\AA . The Zeeman splitting will destroy superconductivity when its magnitude $\mu_B H$ is of the order of $k_B T_c$, which corresponds to $H \approx 10T$ for Pb. Since these fields have the same order of magnitude, we will need to consider both effects.

We first examine the orbital effect. The magnetic field causes the eigenvalues of the Cooperon operator to change from the zero-field values

$$Dq^2 = D \left[\left(\frac{2\pi n}{L} \right)^2 + \left(\frac{\pi p}{a} \right)^2 \right], \quad n = 0, \pm 1, \pm 2 \dots, \quad p = 0, 1, 2 \dots \quad (25)$$

to the eigenvalues, λ , of the minimally coupled Cooperon operator

$$D(-i\nabla + 2e\mathbf{A})^2\psi(x, y) = D \left[\left(-i\frac{\partial}{\partial x} + 2eHy \right)^2 + \left(-i\frac{\partial}{\partial y} \right)^2 \right] \psi(x, y) = \lambda\psi(x, y). \quad (26)$$

where we have chosen the gauge $\mathbf{A} = (-Hy, 0, 0)$. The eigenfunctions $\psi(x, y)$ must satisfy zero-gradient boundary conditions on the sides of the wire, $y = \pm a/2$, and periodic boundary conditions at the ends of the wire, $x = 0, L$. The solution has separable form

$$\psi(x, y) = \phi_{q_n, p}(y)e^{iqx}, \quad q_n = \frac{2\pi n}{L}, \quad n = 0, \pm 1, \pm 2 \dots \quad (27)$$

where $\phi_{q_n, p}$ satisfies the equation

$$D \left[-\frac{d^2}{dy^2} + (q + 2eHy)^2 \right] \phi_{q_n, p}(y) = \lambda_{q_n, p} \phi_{q_n, p}(y), \quad \frac{d\phi_{q_n, p}}{dy}(\pm a/2) = 0, \quad (28)$$

and $p = 0, 1, 2 \dots$ labels the eigenvalues in ascending order.

To solve this eigenvalue problem numerically, we convert it into a matrix diagonalization problem by working in a truncated function space spanned by eigenfunctions of the zero-field problem. The lowest eigenvalue, $\lambda_{0,0}$, equals $2/\tau_H$, where $1/\tau_H$ is the magnetic dephasing rate which appears in the Abrikosov-Gor'kov equation²⁰ for $T_c(H)$. There are two asymptotic limits where $1/\tau_H$ is easily determined: the 2D limit, where the problem becomes that of a simple harmonic oscillator, with $1/\tau_H = DeH$; and the 1D limit, where the eigenfunction is simply a constant, and hence (using perturbation theory) $1/\tau_H = De^2 H^2 a^2/6$. The 2D to 1D crossover occurs when the width, a , is of the order of the magnetic length, $L_H = (\hbar/eH)^{1/2}$, which occurs at the field $H_0 = \hbar/ea^2$. At larger magnetic fields the

cyclotron orbit of the electron lies entirely within the wire, and hence we are in the 2D limit; at smaller magnetic fields the electron hits the sides of the wire before completing a cyclotron orbit, and hence we are in the 1D limit. To summarise,

$$\frac{1}{\tau_H} = \begin{cases} DeH & H \gg H_0 \quad 2\text{D} \\ De^2H^2a^2/6 & H \ll H_0 \quad 1\text{D} \end{cases} \quad (29)$$

These eigenvalues then enter into our equations for the pair propagator in two ways: (i) the term Dq^2 in the q -dependent pair propagator is replaced by the lowest eigenvalue $\lambda_{0,0}$; (ii) sums over functions of Dq^2 in diagrams which involve Cooperonic ladders (e.g. diagrams 2 and 4 in Fig. 1(c)) are replaced by sums over $\lambda_{q_n,p}$. Obviously sums over functions of Dq^2 in diagrams which involve diffusion ladders (e.g. diagrams 1 and 3 in Fig. 1(c)) remain unchanged. It is numerically very expensive to perform the sums over all the eigenvalues, so we would like to see how important it is to use these eigenvalues in any sums. To answer this question we again use perturbation theory as our testing ground. We perform the Cooperonic sum in two different ways – both correctly, and by replacing it by the corresponding diffusion sum. In both cases we still make the replacement of Dq^2 by $\lambda_{0,0} = 2/\tau_H$. The perturbative equations are then

$$\begin{aligned} \frac{\delta P_1}{N(0)} &= -\frac{t}{2} \sum_{m=1}^M \left\{ 2 \left[\psi \left(\frac{1}{2} + m + \alpha \right) - \psi \left(\frac{1}{2} + \alpha \right) \right] I_2(m) + \left[\psi' \left(\frac{1}{2} + \alpha \right) - \psi' \left(\frac{1}{2} + m + \alpha \right) \right] I_1(m) \right\} \\ \frac{\delta P_2}{N(0)} &= +\frac{t}{2} \sum_{m=1}^M \left[\psi' \left(\frac{1}{2} + \alpha \right) - \psi' \left(\frac{1}{2} + m + \alpha \right) \right] C_1(m) \\ \frac{\delta P_3}{N(0)} &= -t \sum_{m=1}^M \frac{1}{m+2\alpha} \left[\psi \left(\frac{1}{2} + m + \alpha \right) - \psi \left(\frac{1}{2} + \alpha \right) \right] (I_1(m) + 2\alpha I_2(m)) \\ \frac{\delta P_4}{N(0)} &= -t \sum_{m=1}^M \frac{1}{m+2\alpha} \left[\psi \left(\frac{1}{2} + m + \alpha \right) - \psi \left(\frac{1}{2} + \alpha \right) \right] C_1(m) \end{aligned} \quad (30)$$

where $\alpha = 1/2\pi T\tau_H$. The diffusive sums $I_1(m)$ and $I_2(m)$ are defined as in Eqn. (15) except that here we perform the momentum sums in the longitudinal direction *exactly* to give

$$\begin{aligned} I_1(m) &= \frac{4\pi D}{aL} \sum_q \frac{1}{Dq^2 + 2\pi Tm} = \frac{L_T^2}{\pi La} \sum_{n=-n_0}^{n_0} \sum_{k=0}^{k_0} \frac{1}{\left[m + \left(\frac{kL_T}{2a} \right)^2 + \left(\frac{nL_T}{L} \right)^2 \right]} \\ I_2(m) &= \frac{4\pi D}{aL} \sum_q \frac{2\pi T}{(Dq^2 + 2\pi Tm)^2} = \frac{L_T^2}{\pi La} \sum_{n=-n_0}^{n_0} \sum_{k=0}^{k_0} \frac{1}{\left[m + \left(\frac{kL_T}{2a} \right)^2 + \left(\frac{nL_T}{L} \right)^2 \right]^2} \end{aligned} \quad (31)$$

and the Cooperonic sum, C_1 , which is now distinct from I_1 , is given by

$$C_1(m) = \frac{4\pi D}{aL} \sum_q \frac{1}{Dq^2 + 2\pi Tm} = \frac{L_T^2}{\pi La} \sum_{n=-n_0}^{n_0} \sum_{k=0}^{k_0} \frac{1}{\left[m + \lambda_{nk}/2\pi T \right]}. \quad (32)$$

We found essentially no difference between using the correct C_1 , or replacing it by I_1 , over a wide range of magnetic fields. It follows that the only replacement we need to make is of Dq^2 by $\lambda_{0,0}$, which greatly reduces the numerical cost.

Let us next consider the effect of the Zeeman splitting. This leads to changes in both the mean field and perturbative terms, and we will show that only the former effect is important. To do this we will evaluate the mean field pair polarization function and the first-order perturbation correction, δP , both with and without Zeeman splitting. We find that the latter is essentially unaffected. To treat the Zeeman effect, we need formulas for the Cooperon impurity ladder and Hikami boxes²¹, where we note that the boxes in diagrams 1 and 3 of Fig. 1(c) will give different contributions. The non-zero elements of the spin-dependent Cooperon ladder, $C_{\alpha\beta\gamma\delta}$, are

$$C_{\uparrow\uparrow\downarrow\downarrow} = \frac{1}{2\pi N(0)\tau^2} \frac{1}{Dq^2 + |\omega| + |\omega'| - 2i\Delta}, \quad C_{\downarrow\downarrow\uparrow\uparrow} = \frac{1}{2\pi N(0)\tau^2} \frac{1}{Dq^2 + |\omega| + |\omega'| + 2i\Delta} = C_{\uparrow\uparrow\downarrow\downarrow}^* \quad (33)$$

where $\Delta = \mu_B H$ is the Zeeman splitting. The appropriate spin combination which occurs in an s-wave pair propagator is $C_{\uparrow\uparrow\downarrow} + C_{\downarrow\downarrow\uparrow} = 2\Re C_{\uparrow\downarrow\uparrow}$. This leads to the mean field formula for T_c ,

$$\ln\left(\frac{T_c}{T_{c0}}\right) = \psi\left(\frac{1}{2}\right) - \Re e\left[\psi\left(\frac{1}{2} + \kappa\right)\right] \quad (34)$$

where $\beta = \Delta/2\pi T_c = \mu_B H/2\pi T_c$, and $\kappa = \alpha - i\beta$. To calculate the first-order pair polarization terms δP_{1-4} , we note that: (a) the diffusion ladders on Coulomb vertices are unchanged; (b) Cooperon ladders pick up an extra $\mp 2i\Delta$ as described above; (c) the Hikami box in δP_1 picks up an extra $\mp 2i\Delta$, whilst the box in δP_3 is unaffected. This leads to the formulas

$$\begin{aligned} \frac{\delta P_1}{N(0)} &= -\frac{t}{2}\Re e \sum_{m=1}^M \left\{ 2\left[\psi\left(\frac{1}{2} + m + \kappa\right) - \psi\left(\frac{1}{2} + \kappa\right)\right] I_2(m) + \left[\psi'\left(\frac{1}{2} + \kappa\right) - \psi'\left(\frac{1}{2} + m + \kappa\right)\right] I_1(m) \right\} \\ \frac{\delta P_2}{N(0)} &= +\frac{t}{2}\Re e \sum_{m=1}^M \left[\psi'\left(\frac{1}{2} + \kappa\right) - \psi'\left(\frac{1}{2} + m + \kappa\right)\right] \bar{C}_1(m) \\ \frac{\delta P_3}{N(0)} &= -t\Re e \sum_{m=1}^M \frac{1}{m + 2\kappa} \left[\psi\left(\frac{1}{2} + m + \kappa\right) - \psi\left(\frac{1}{2} + \kappa\right)\right] (I_1(m) + 2\alpha I_2(m)) \\ \frac{\delta P_4}{N(0)} &= -t\Re e \sum_{m=1}^M \frac{1}{m + 2\kappa} \left[\psi\left(\frac{1}{2} + m + \kappa\right) - \psi\left(\frac{1}{2} + \kappa\right)\right] \bar{C}_1(m) \end{aligned} \quad (35)$$

where $I_1(m)$ and $I_2(m)$ are the same as before, whilst

$$\bar{C}_1(m) = \frac{4\pi D}{aL} \sum_q \frac{1}{Dq^2 + 2\pi Tm - 2i\Delta} = \frac{L_T^2}{\pi aL} \sum_{n=-n_0}^{n_0} \sum_{k=0}^{k_0} \frac{1}{\left[m + 2\kappa + \left(\frac{kL_T}{2a}\right)^2 + \left(\frac{nL_T}{L}\right)^2\right]} \quad (36)$$

Calculating the δP_{1-4} as above, or with β set to zero, we find essentially no difference over a wide range of magnetic fields until we get to widths of order 10\AA . It follows that we only need consider the Zeeman splitting at the mean field level. Even this is a small effect, only noticeable for wires narrower than about 150\AA .

Let us finally perform calculations of T_c using the resummation technique. From the discussions above, we now know that to include magnetic field effects we need only replace Dq^2 in Cooperons by $2/\tau_H$, which must be calculated numerically, and include the Zeeman splitting at the mean field level. The Cooperon denominator $Dq^2 + 2|\epsilon_m|$ then becomes $2|\epsilon_m| + 2/\tau_H - 2i\Delta$, and hence $\hat{\epsilon}_{nm} = (n + 1/2 + \kappa)\delta_{nm}$, which is now complex. Because the two spin configurations which occur in an s-wave pair propagator are complex conjugates of each other, we end up taking the real part of the complex matrix equation. The equation for Λ_{nm} becomes

$$\Lambda_{nm} = \begin{cases} I_1(n + m + 1 + 2\alpha) & \epsilon_n \epsilon_m > 0 \\ I_1(n + m + 1 + 2\alpha) + 2I_2(n + m + 1 + 2\alpha) & \epsilon_n \epsilon_m < 0 \end{cases} \quad (37)$$

where we have not included the Zeeman effect as we have shown this to be much smaller in perturbation theory. We are now in a position to calculate transition temperature, T_c , as a function of resistance per square, R_{\square} , wire width, a , and applied magnetic field, H . This obviously leads to a wide choice of ways to present results. Experimentally one would probably vary magnetic field on a sample of fixed width and thickness, and so we plot $T_c(H)$ for different a and fixed R_{\square} on the same graph, and present graphs for $R_{\square} = 0, 500, 1000\Omega$. The results are shown in Fig. 8.

V. DISCUSSION AND CONCLUSIONS

In this paper we have considered the effect of localization and interaction on transition temperature in ultranarrow superconducting wires. Our main conclusion is that, in contradiction to previous work, theory and experiment do not agree in a quantitative fashion. The experimental data seems to show a very sudden crossover from 2D to 1D behavior when the wire width becomes of the order of the thermal length, whilst theory predicts a smooth crossover. Indeed, when plotted as the additional relative suppression of transition temperature due to finite width, the experimental data falls on two curves – one for the 2D film and 1000\AA wire; the other for the 580\AA , 350\AA and 250\AA wires. However, this conclusion is based on a single experiment, as this is the only experiment which shows any consistent

trend with wire width. More experimental data is obviously needed to investigate this further. Given the difficulty in fabricating these wires, we suggest that the magnetic field dependence of transition temperature be measured in future experiments. We have therefore made predictions for magnetic field dependence of transition temperature in wires of varying width and resistance in the hope that in the future such measurements will be made.

Our work is based on the resummation technique developed by Oreg and Finkel'stein, which is a very powerful method of going beyond perturbation theory, and hence giving believable results at strong disorder. The main reason our results differ from theirs is the different set of boundary conditions we use for the superconducting wavefunction on the sides of the wire. The suppression of the transition temperature is very sensitive to boundary conditions, probably due to the different relative weights of the zero momentum mode. We have used the physically correct zero-gradient boundary conditions in our work. This unexpected strong dependence of results on boundary conditions led us to worry about all details of the calculation. We therefore also investigated the effects of using a featureless Coulomb interaction instead of the exact one, ignoring self-energy contributions, and solving the OF matrix equation exactly instead of using an approximate method. We found that it is legitimate to use a featureless Coulomb interaction and ignore self-energy contributions, but that our matrix equations should be solved by exact diagonalization (which in any case is no more difficult).

In our calculations of the magnetic field dependence of transition temperature, we find that the orbital effect is the most important, and can be treated by replacing the Dq^2 terms in the momentum dependent pair propagator, $L(q, 0)$, by twice the magnetic dephasing rate, $2/\tau_H$. The latter is the lowest eigenvalue of the minimally coupled Cooperon operator, and must be found numerically. The Zeeman splitting is found to have a non-negligible effect only at the mean field level, and even this effect is small. The perturbative term only becomes important in very narrow wires (of order 10\AA), which cannot currently be fabricated.

ACKNOWLEDGEMENTS

We thank I. Aleiner, A. Clerk, A.M. Finkel'stein, I.V. Lerner, Y. Oreg and M. Steiner for helpful discussions. RAS acknowledges support from the Nuffield Foundation and the UK EPSRC under Grant No GR/M98975. BSH acknowledges support from the UK EPSRC. VA is supported by the US National Science Foundation under Grant No DMR-9805613.

APPENDIX A: DETAILS OF SOME MOMENTUM SUMS

In this appendix we derive expressions for the quantities $I_1(m)$ and $I_2(m)$ defined in Eqn. (15) as

$$\begin{aligned} I_1 &\equiv \frac{4\pi D}{aL} \sum_{q'} \frac{1}{Dq'^2 + |\omega_m|} \\ I_2 &\equiv \frac{4\pi D}{aL} \sum_{q'} \frac{2\pi T}{(Dq'^2 + |\omega_m|)^2} \end{aligned} \quad (\text{A1})$$

In two dimensions the sum becomes an integral, and cutting off in a circularly symmetric manner,

$$\frac{1}{aL} \sum_{q'} = \int_0^{Dq'^2=1/\tau} \frac{2\pi q' dq'}{(2\pi)^2} = \int_0^{1/\tau} \frac{d(Dq'^2)}{4\pi D}, \quad (\text{A2})$$

we obtain the results

$$I_1(m) = \ln\left(\frac{M}{m}\right), \quad I_2(m) = \frac{1}{m}. \quad (\text{A3})$$

In quasi-1D wires we replace the integral in the transverse direction by a sum, so that $I_1(m)$ becomes

$$\begin{aligned} I_1(m) &= 4\pi D \frac{1}{a} \sum_{q'_a} \frac{1}{2\pi} \int_0^{Dq'^2_L=1/\tau} \frac{dq'_L}{Dq'^2_L + Dq'^2_a + 2\pi Tm} \\ &= \frac{4}{a} \sum_{q'_a} \frac{1}{\sqrt{q'^2_a + \frac{2\pi Tm}{D}}} \tan^{-1} \left[\frac{1/\sqrt{D\tau}}{\sqrt{q'^2_a + \frac{2\pi Tm}{D}}} \right], \end{aligned} \quad (\text{A4})$$

and $I_2(m)$ can be found by differentiating the above with respect to m and dividing by $-2\pi T$. Substituting in the three types of boundary condition listed in Table 1 yields

$$I_1(m) = \begin{cases} \frac{2}{\pi} \sum_{p=-p_0}^{p_0} (p^2 + mA^2)^{-\frac{1}{2}} \tan^{-1} \left[\frac{p_0}{\sqrt{p^2 + mA^2}} \right] & \text{PBC} \\ \frac{4}{\pi} \sum_{p=0}^{2p_0} (p^2 + 4mA^2)^{-\frac{1}{2}} \tan^{-1} \left[\frac{2p_0}{\sqrt{p^2 + 4mA^2}} \right] & \text{ZGBC} \\ \frac{4}{\pi} \sum_{p=0}^{p_0} (p^2 + mA^2)^{-\frac{1}{2}} \tan^{-1} \left[\frac{p_0}{\sqrt{p^2 + mA^2}} \right] & \text{OFBC} \end{cases} \quad (\text{A5})$$

and

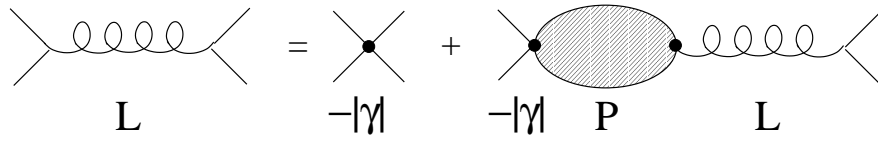
$$I_2(m) = \begin{cases} \frac{A^2}{\pi} \sum_{p=-p_0}^{p_0} (p^2 + mA^2)^{-\frac{3}{2}} \left(\tan^{-1} \left[\frac{p_0}{\sqrt{p^2 + mA^2}} \right] + \frac{p_0 \sqrt{p^2 + mA^2}}{p^2 + (m+M)A^2} \right) & \text{PBC} \\ \frac{8A^2}{\pi} \sum_{p=0}^{2p_0} (p^2 + 4mA^2)^{-\frac{3}{2}} \left(\tan^{-1} \left[\frac{2p_0}{\sqrt{p^2 + 4mA^2}} \right] + \frac{2p_0 \sqrt{p^2 + mA^2}}{p^2 + 4(m+M)A^2} \right) & \text{ZGBC} \\ \frac{2A^2}{\pi} \sum_{p=0}^{p_0} (p^2 + mA^2)^{-\frac{3}{2}} \left(\tan^{-1} \left[\frac{p_0}{\sqrt{p^2 + mA^2}} \right] + \frac{p_0 \sqrt{p^2 + mA^2}}{p^2 + (m+M)A^2} \right) & \text{OFBC} \end{cases} \quad (\text{A6})$$

where $A = a/L_T$ is a dimensionless width, the ratio of the wire width to the thermal length.

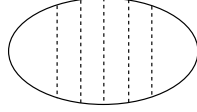
- ¹ J.M. Graybeal, P.M. Mankiewich, R.C. Dynes and M.R. Beasley, *Phys. Rev. Lett.* **59**, 2697 (1987).
² F. Sharifi, A.V. Herzog and R.C. Dynes, *Phys. Rev. Lett.* **71**, 428 (1993).
³ P. Xiong, A. V. Herzog and R. C. Dynes, *Phys. Rev. Lett.* **78**, 927 (1997).
⁴ A. Bezryadin, C.N. Lau and M. Tinkham, *Nature* **404**, 971 (2000).
⁵ B. Reulet, *Bull. Am. Phys. Soc.* **45**, 486 (2000).
⁶ D.B. Haviland, Y. Liu and A.M. Goldman, *Phys. Rev. Lett.* **62**, 2180 (1989).
⁷ S. Maekawa and H. Fukuyama, *J. Phys. Soc. Jpn.* **51**, 1380 (1982).
⁸ A.M. Finkel'stein, *JETP Lett.* **45**, 46 (1987).
⁹ R.A. Smith, M.Y. Reizer and J.W. Wilkins, *Phys. Rev. B* **51**, 6470 (1995).
¹⁰ A. Schmid, *Z. Phys.* **259**, 421 (1973).
¹¹ D. Belitz, *Phys. Rev. B* **35**, 1636 (1987); *ibid* **35**, 1651 (1987).
¹² B.L. Altshuler, A.G. Aronov and P.A. Lee, *Phys. Rev. Lett.* **44**, 1288 (1980).
¹³ J.M. Valles Jr, R.C. Dynes and J.P. Garno, *Phys. Rev. B* **40**, 6680 (1989).
¹⁴ R.A. Smith and V. Ambegaokar, *Phys. Rev. B* to be published.
¹⁵ Y. Oreg and A.M. Finkel'stein, *Phys. Rev. Lett.* **83**, 191 (1999).
¹⁶ M. Steiner and R.A. Smith, e-print cond-mat 0006160.
¹⁷ P.G. de Gennes, "Superconductivity of Metals and Alloys", (Addison-Wesley, Redwood City, 1989), p227.
¹⁸ R.A. Smith, B.S. Handy and V. Ambegaokar, *Phys. Rev. B* **61**, 6352 (2000).
¹⁹ A.M. Clogston, *Phys. Rev. Lett.* **9**, 266 (1962); B.S. Chandrasekhar, *Appl. Phys. Lett.* **1**, 7 (1962).
²⁰ A.A. Abrikosov and L.P. Gor'kov, *Sov. Phys. JETP* **12**, 1243 (1961).
²¹ S. Hikami, *Phys. Rev. B* **24**, 2671 (1981).

Type	Definition	Momenta, q_a	Details of sum over p
Periodic	$\psi(x+a) = \psi(x)$	$\frac{2\pi p}{a}$	$\sum_{p=-p_0}^{p_0}$
Zero-Gradient	$\psi'(x = \pm a/2) = 0$	$\frac{\pi p}{a}$	$\sum_{p=0}^{2p_0}$
Oreg-Finkel'stein		$\frac{2\pi p}{a}$	$2 \sum_{p=0}^{p_0}$

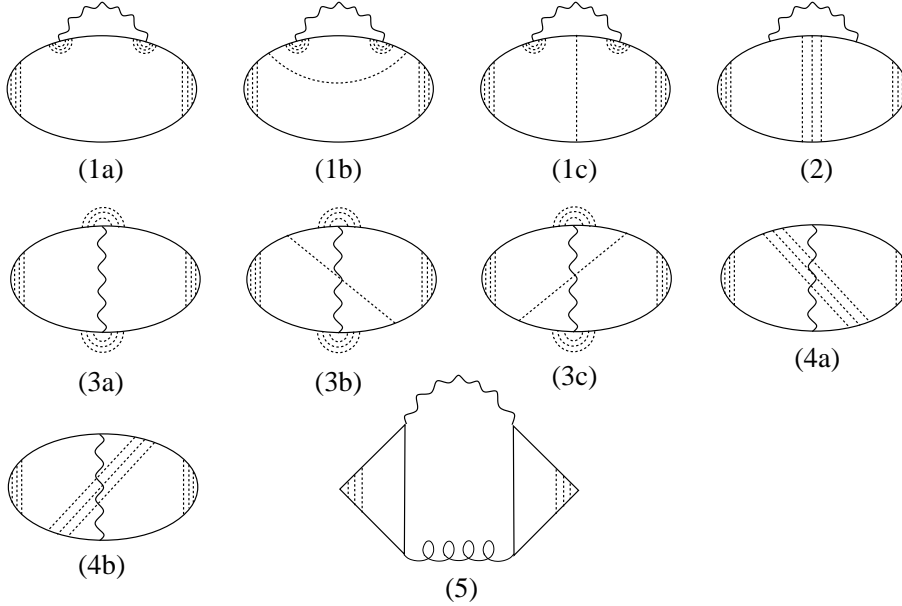
TABLE I. Details of the three types of boundary condition discussed in the text. The upper cut-off in momentum is given by $Dq_a^2 = 1/\tau$, so that $p_0 = a/2\pi\sqrt{D\tau} = \sqrt{M}(a/L_T)$ where $L_T = \sqrt{2\pi D/T}$ is the thermal length and $M = 1/2\pi T\tau$. Note that if we replace a by $a/2$ in the zero-gradient sums we obtain the Oreg-Finkel'stein ones.



(a)



(b)



(c)

FIG. 1. The diagrams needed to calculate the first-order perturbative correction to the pair-propagator $L(q, 0)$. (a) Definition of pair propagator, $L(q, 0)$, in terms of the pair polarization function, $P(q, 0)$, and the 4-point BCS interaction $-|\gamma|$. (b) Zeroth-order (mean-field) polarization function, $P_0(q, 0)$, in a dirty superconductor. The solid lines are electron Green functions; the dashed lines are impurity lines. (c) First-order perturbative correction to pair polarization function, $\delta P(q, 0)$. The wiggly line is the screened Coulomb interaction.

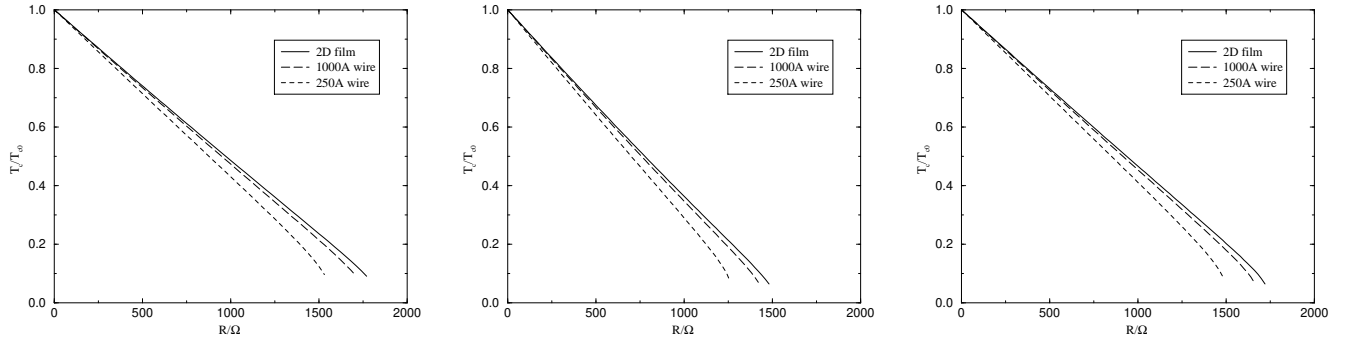


FIG. 2. Comparison of three approaches to perturbation theory for the case of zero-gradient boundary conditions. In the left plot we calculate the first-order perturbative correction to transition temperature correctly. In other words we use the correctly screened Coulomb potential and all five diagrams in Fig. 1(c). In the other two plots we use a featureless Coulomb interaction and a restricted set of diagrams. The middle plot includes diagrams 1–4 (i.e. both self-energy and pseudopotential diagrams), whilst the right plot includes only diagrams 3 and 4 (i.e. only pseudopotential diagrams). The curves plotted are for 2D films and wires of width 1000\AA and 250\AA . We see that we are justified in using any of the approaches since the slight difference between them can be absorbed by fitting the initial slope in the 2D curve, which sets the value of the upper cut-off M .

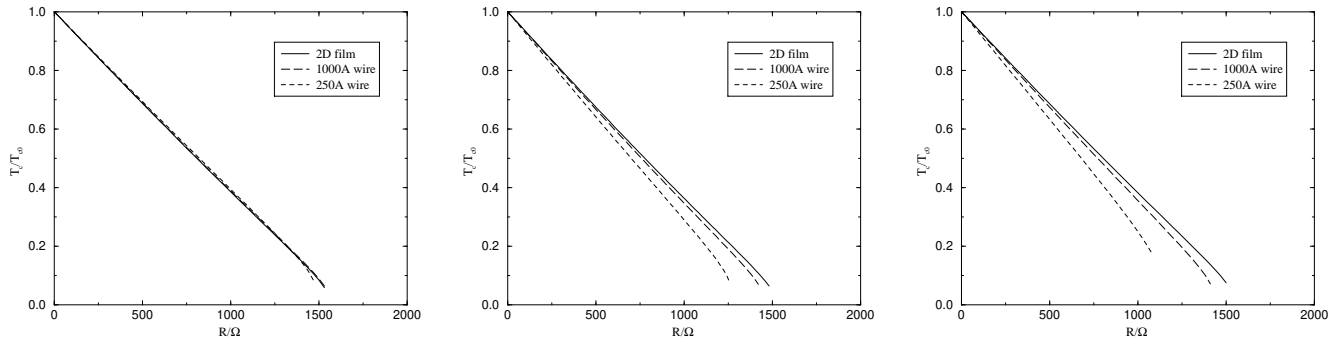


FIG. 3. Comparison of the effect of different types of boundary condition on perturbation theory. The plots from left to right use periodic, zero-gradient and Oreg and Finkel'stein's boundary conditions respectively. The curves plotted are for 2D films and wires of width 1000\AA and 250\AA , with a thermal length $L_T = 300\text{\AA}$. We see that the type of boundary condition used has a large effect on predictions, and we must therefore be careful to use the correct one. Note that the Oreg-Finkel'stein curves identical to the zero-gradient results for half the wire width.

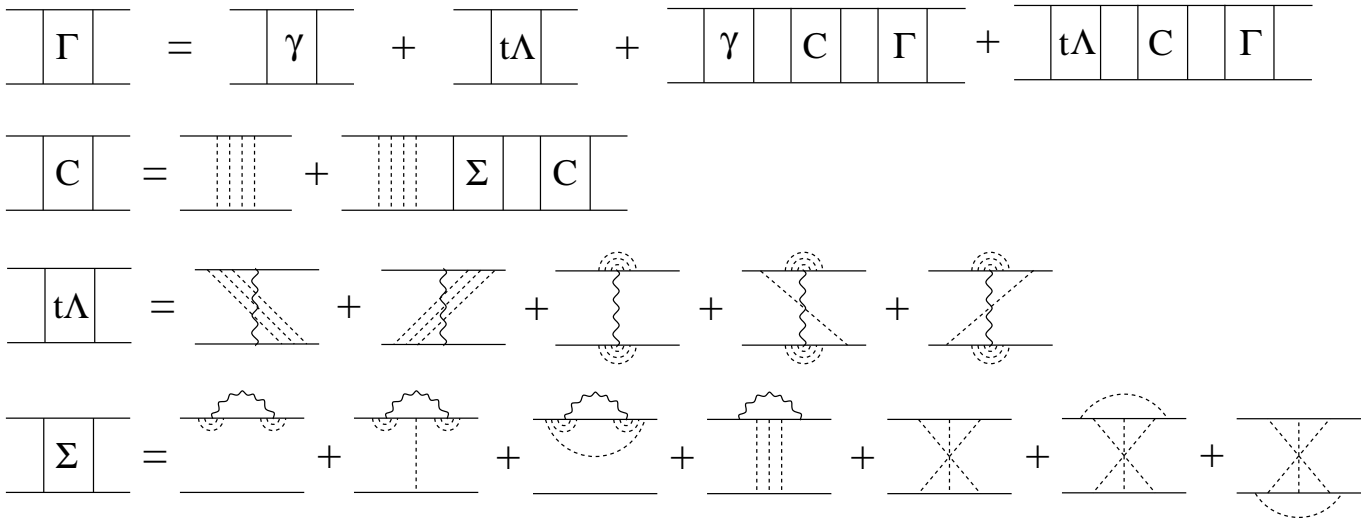


FIG. 4. Diagrammatic equation for the pair amplitude matrix $\Gamma(\epsilon_n, \epsilon_l)$. Block γ is the BCS interaction. Block $t\Lambda$ is the correction to the effective interaction caused by the interplay of Coulomb interaction and disorder. Block Σ is the correction to the bare Cooperon ladder caused by Coulomb interaction and disorder, which yields a negligible contribution and is thus ignored in our numerical calculations.

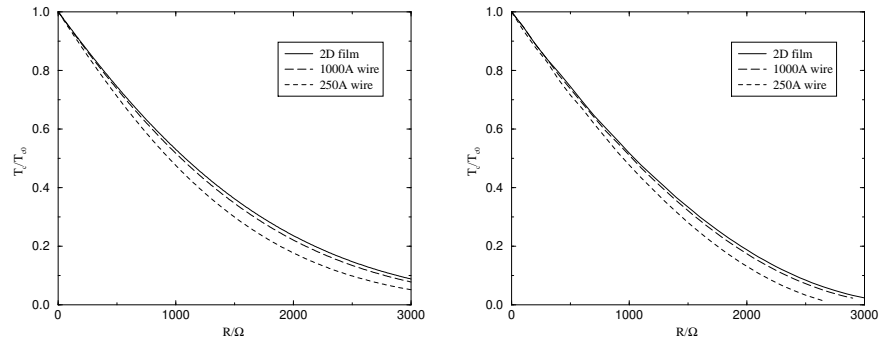


FIG. 5. Comparison of matrix perturbation theory (left) and exact diagonalization (right). We see that the two predictions agree at low values of resistance, but deviate at higher values. The exact method predicts a larger suppression.

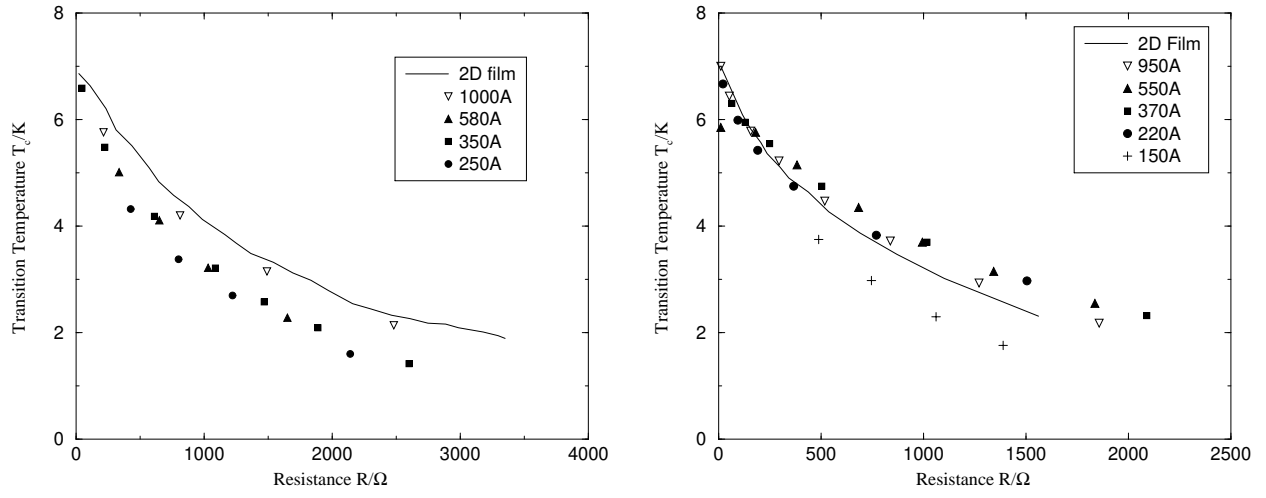


FIG. 6. Experimental data in the form of transition temperature vs resistance per square, $T_c(R_{\square})$, for wires of differing width and a reference 2D film. The data on the left is from Xiong et al (1997); the data on the right is from Sharifi et al (1993). We see that only the data of Xiong et al shows a consistent trend of T_c with decreasing width.

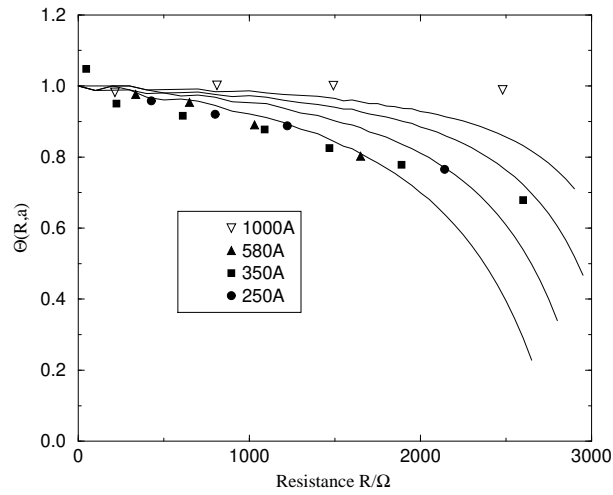


FIG. 7. Comparison of theory (solid lines) and experiment (symbols) for the data of Xiong et al. The data is plotted in the form of the scaled transition temperature, $\Theta(R_{\square}, a)$, vs the resistance per square, R_{\square} . The theory used is the one we have argued to be correct – resummation technique solved by exact diagonalization using zero-gradient boundary conditions. We see that theory predicts the correct order of magnitude of the effect, but that the detailed fit is not particularly good.

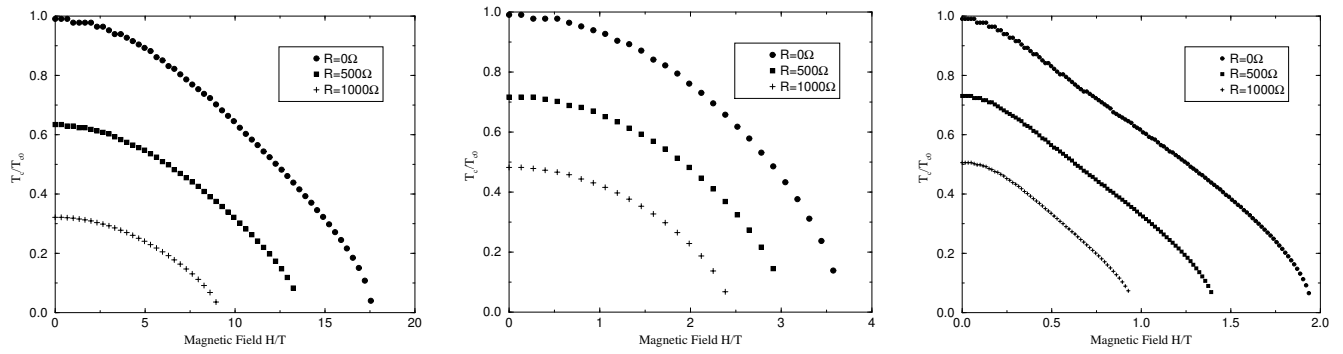


FIG. 8. Theoretical predictions for the transition temperature as a function of applied magnetic field for wires of differing resistance per square. The plots from left to right are for wires of width 50\AA , 250\AA and 1000\AA respectively.